Statistics of Thermal Plasma Parameters and Non-Thermal X-Ray Spectra of Solar Flares with Helioseismic Response

I. N. Sharykin^{a,*}, I. V. Zimovets^a, and A. G. Kosovichev^b

^aSpace Research Institute of Russian Academy of Sciences, Moscow, 117997 Russia ^bNew Jersey Institute of Technology, Newark, USA *e-mail: ivan.sharykin@phystech.edu Received July 13, 2023; revised August 17, 2023; accepted August 28, 2023

Abstract—We present the results of statistical analysis of various thermal plasma parameters and non-thermal X-ray spectra of helioseismically active (producing "sunquakes") solar flares of the 24th solar cycle up to February 2014. Two samples of flares are compared: with helioseismic activity in the form of sunguakes and a sample of flares without photospheric disturbances. The dependences of the considered flare parameters on the energy of helioseismic disturbances are also investigated. Quantitative parameters of solar flares are taken from the statistical work of the Global Energetics series by Markus Ashwanden in 2014–2019. We consider thermodynamic plasma parameters derived from the analysis of RHESSI X-ray spectra and differential emission measure (from AIA EUV images), as well as the characterization of non-thermal X-ray spectra from RHESSI. Statistical analysis confirmed that helioseismically active solar flares are characterized by significantly larger fluxes of non-thermal X-ray emission compared to flares without photospheric disturbances. A good linear relationship between helioseismic energy and the total flux of non-thermal X-ray radiation and the total energy of accelerated electrons is found. It is shown that the power-law index of the nonthermal X-ray spectrum is not the parameter by which one can separate the two groups of flares under consideration. The analysis of the X-ray thermal spectra shows a slight difference between the flares with the sunsets.

Keywords: solar flares, helioseismic waves, sunquakes, X-ray emission, nonthermal electrons, photosphere, ultraviolet emission

DOI: 10.1134/S1063772923110094

1. INTRODUCTION

A solar flare, manifesting itself in all ranges of the electromagnetic spectrum, is a unique natural laboratory of plasma physics, provided to us by nature for comprehensive research. Both modern observational and theoretical studies of flares are devoted to the most diverse aspects of their energy release: magnetic reconnection, acceleration of charged particles, connection with coronal mass ejections (CMEs), etc. Among the variety of different types of energy release of solar flares, one of the least studied is helioseismic disturbance. It is believed that strong photospheric disturbances during solar flares with optical glow are accompanied by the generation of helioseismic waves, known as "sunquakes". The possibility of such a phenomenon was initially discussed in [1]. Then a theoretical prediction was made [2] based on gas-dynamic numerical simulation. The sunquake was first detected [3] using Dopplerograms from the MDI instrument (Michelson Doppler Imager, [4]) on board the SOHO (Solar Orbital Heliospheric Observatory, [5]).

Typically, helioseismic waves are observed on Dopplerograms (photospheric line-of-sight velocity

maps) as concentric (usually highly anisotropic) waves propagating from the initial photospheric flare disturbances, observed during the impulse phase as bright and dark contrasting groups of pixels. From a physics point of view, sunquakes are acoustic waves passing through the solar convective zone and returning back to the photosphere due to refraction caused by increasing temperature with depth. Wave fronts emerging from inside the Sun into the photosphere are observed on Dopplerograms in the form of packets of traveling circular waves with a characteristic spatiotemporal dependence. Helioseismic disturbances are usually associated with fairly compact disturbances of the photosphere and the appearance of optical radiation near acoustic sources reconstructed by helioseismic (or acoustic) holography [6–9].

A review of the observational properties of sunquakes, the morphology of helioseismic flares and the theory of their generation can be found in articles [10, 11]. We will briefly mention only the main hypotheses for the occurrence of sunquakes. The most discussed mechanism for generating the initial photospheric disturbance is the injection of accelerated electrons into the lower layers of the solar atmosphere. This hypothesis assumes that a sunguake occurs as a result of a reaction to the immediate rapid heating of the photosphere by injected accelerated electrons [2], which is confirmed by the close temporal and spatial connection of sunguake sources with sources of hard X-ray radiation [for example, 12–14]. Recent helioseismic modeling of sunquakes by [15] showed that at least half of the events studied are consistent with the electron beam hypothesis. Accelerated protons can be an even more powerful agent for initiating sunquakes [16]. It is possible that the effect of heating the photosphere by ultraviolet radiation from a flare can also cause a pressure disturbance necessary for the generation of sunquakes waves [10]. Another alternative hypothesis assumes that the momentum of the photospheric plasma can be transferred due to the dynamics of the pressure gradient due to the eruption of a magnetic flux rope (for example, [17, 18]) or due to the Lorentz force impulse, which can be stimulated by a change in the magnetic field in the lower part of the solar atmosphere [19–23]. It was discussed in [24, 25] that the rapid dissipation of electric currents in the lower atmosphere can also explain the occurrence of sunquakes. It is possible that different events may be caused by different mechanisms, or that the described mechanisms may act together and their contribution may also change during the progression of the flare.

Despite the presence of a number of hypotheses based on observational material and a small number of models, we state the fact that the nature of sunguakes is not fully understood. This is due to several aspects. Firstly, there are virtually no detailed theoretical models for the generation of sunquakes. Secondly, observational material on helioseismically active solar flares is relatively poor and sometimes contradictory in comparison with other actively studied aspects of the energy release of solar flares. In reality, all observational work is usually devoted to fragmentary studies of individual events. There have been virtually no statistical studies of the properties of solar flares accompanied by sunguakes. However, today such a study is possible thanks to the availability of several catalogs of helioseismically active solar flares. Moreover, there are the first results of statistical studies that are important for understanding the nature of sunquakes.

The first catalogs of helioseismically active solar flares were presented in [9] and [26] for the 23rd and 24th solar cycles (until February 2014). The catalogs for these cycles list 23 and 18 helioseismic events, respectively; in the first work, only flares with observed hard X-ray radiation above 50 keV were considered (according to the RHESSI (Reuven Ramaty High Energy Solar Spectroscopic Imager) catalog, [27]). In [28], 60 powerful flashes (with X-ray GOES class above M5) in the 24th solar cycle were analyzed by acoustic holography to search for sunquakes using the helioseismic holography method [8]. A total of 24 flares were considered seismically active. However,

in this work, no statistical studies of any flare parameters were carried out.

The most complete catalog of helioseismically active solar flares of the 24th cycle is described in [29] (hereinafter we will refer to this catalog as SO24), which used observational data from the Helioseismic Magnetic Imager (HMI, [30]) instrument on board the space Solar Dynamics Observatory (SDO, [31]). This study identified 94 flares with reliably identified sunguakes and a small group of potential candidates. A statistical study of GOES observations of the total soft X-ray flux in the 1–8 Å channel was also carried out and showed that the power of sunguakes correlates more with the maximum derivative of the soft X-ray flux rather than the X-ray (GOES) class of the flare. This fact indirectly indicates that the nature of sunquakes is associated with the presence of populations of accelerated electrons in the flare region. This conclusion was made on the basis of the Neupert effect [32, 33], which states that the derivative of the soft thermal X-ray flux correlates with the hard X-ray flux. This effect results from the heating of the chromosphere by the electron beam, and non-thermal X-rays are generated by the electron beam as a result of Coulomb collisions with plasma ions [34]. The beam heats the chromospheric plasma to coronal temperatures, causing its evaporation and an increase in the fluxes of thermal soft X-ray radiation in the corona, as follows from radiation hydrodynamics modeling [35–38]. However, real information about accelerated electrons cannot be obtained only by using indirect effects. Analysis of the spectra of hard X-rays or microwave radio emission is required.

To date, there is only one known attempt to statistically analyze X-ray spectra in relation to helioseismically active flares [39]. This paper presents a comparative analysis of the non-thermal energy of two samples of powerful (GOES class in the range M7.2– X6.9) flares: 12 flares with sunquakes, 8 flares without photospheric disturbances. The work [39] states that helioseismically active flares are characterized by higher integral energies of non-thermal electrons (non-thermal energy) above 300 keV, while the total non-thermal energy of electrons with energies above 50 keV on average is practically the same in these two groups. In other words, flares with sunquakes are "harder" in spectra with a predominance of highenergy accelerated electrons. However, from our point of view, the statistics in this work are quite poor and are reduced only to a comparison of the rigidity of the spectrum of accelerated particles without considering other parameters obtained from the analysis of X-ray radiation. In addition, comparison of the histograms in this work does not allow us to draw a clear conclusion about the difference in the spectra at high ener-

This article is devoted to a detailed statistical study of helioseismically active solar flares from the SQ24

catalog. The main goal is to obtain new information about the properties of flares with sunquakes, necessary for understanding the physics of this phenomenon. In particular, we are going to support with new observational statistical data the most natural (in our subjective opinion) hypothesis about the generation of sunquakes by accelerated electrons. Within the framework of this work, two main tasks are solved:

- (1) Statistical study of the thermodynamic parameters of solar flares with sunquakes based on X-ray observations based on RHESSI data and based on the analysis of the differential emission measure (DEM) obtained from observations of extreme ultraviolet radiation (EUV) using the Atmospheric Imaging Assembly (AIA, [40]) instrument on board SDO.
- (2) Statistical study of the parameters of non-thermal X-ray spectra of solar flares with sunquakes based on observations of X-ray radiation according to RHESSI data. Determination of non-thermal energies of solar flares.

It is worth noting that the first task does not directly concern the main hypotheses of the generation of sunquakes. The solution to this problem is necessary, first of all, to form a general view of the morphology and thermal response of flares with helioseismic activity. Thermodynamic and non-thermal parameters will be taken from published catalogs of other authors (details in the next section). Each of the two tasks is methodologically split into:

- (1) comparative analysis of flares with sunquakes and without photospheric disturbances (flares with photospheric disturbances do not necessarily produce sunquakes) according to various thermal and nonthermal parameters;
- (2) analysis of correlations between various studied flare parameters and the energy of helioseismic waves, estimated using the acoustic holography method.

The article consists of five sections, not counting the Introduction. The first section briefly describes the SQ24 catalog, as well as the catalogs from which we take the necessary parameters for the two tasks under consideration. Then, the next section examines the statistics of thermal plasma parameters from RHESSI X-ray spectroscopy data. The third, largest section of the article discusses the statistics of parameters of the non-thermal X-ray spectrum based on the same RHESSI data. It also provides statistical data on the non-thermal energy of accelerated particles in the considered groups of flares. The fourth section describes the results of statistical analysis of thermal plasma parameters obtained from the analysis of the DEM according to AIA data. At the end of each of Sections 2-4, we provide lists of the main results of the statistical analyses, to lighten the load on the final section, in which we discuss the main findings and results of the paper.

2. USED DATA AND CATALOGS, SELECTION OF FLARES FOR STATISTICAL ANALYSIS

Let us discuss the main aspects of the work performed on the search for helioseismic flares for the SQ24 catalog [29]. All selected solar flares for the 24th cycle were analyzed for the presence of helioseismic waves using HMI/SDO Dopplerograms using the following methods:

- (1) a visual method based on the creation of films that show the time sequence of difference HMI Dopplerograms filtered in the frequency range of 5–7 MHz;
- (2) a method for constructing time—distance diagrams with various averaging from points where the strongest photospheric disturbances were observed on Dopplerograms;
- (3) reconstruction of maps of helioseismic wave sources using the acoustic holography method [8].

A flare was considered helioseismically active if one of these three methods gave a positive result. A total of 507 solar flares of M and X GOES class were analyzed for the 24th cycle with a distance from the center of the solar disk to 800 arcsec. The number of solar flares with photospheric disturbances visible on Dopplerograms and with optical glow was 181. The number of solar flares with helioseismic disturbances that were recorded by at least one of three methods was 93 (plus 19 candidates) in 35 active areas. Thus, considering the candidates, more than half of the events with photospheric disturbances were accompanied by the generation of helioseismic waves. In this work, we will consider only those helioseismically active flares (80 events) in which it was possible to register acoustic sources using the acoustic holography method. For such flares, we have estimates of the total energy of sunguakes in the frequency range 5–7 MHz. And therefore, for these flares, we will be able to conduct a correlation analysis between the energy of the helioseismic disturbance and various parameters within the framework of the two problems being solved (see Introduction).

The panel (a) of Fig. 1 shows the dependence of the total acoustic energy on the GOES class (maximum X-ray flux in the channel 1-8 Å). Panel (b) of the same figure demonstrates the dependence of the maximum value of the time derivative of the flux of 1-8 Åon the energy of the helioseismic disturbance. All events marked in red and blue on the graphs (the meaning of these colors will be discussed a little below) are real helioseismically active flares, while black corresponds to candidate events in the SQ24 catalog. For clarity, the figures show the values of correlation coefficients for different groups of flares (Pearson and rank correlation) to demonstrate a stronger connection of the derivative with the energy of sunquakes. When candidates for sunguakes are considered, the correlation coefficient becomes lower (0.4 and 0.57 for (a) and (b)). In this article, we will not use candidates

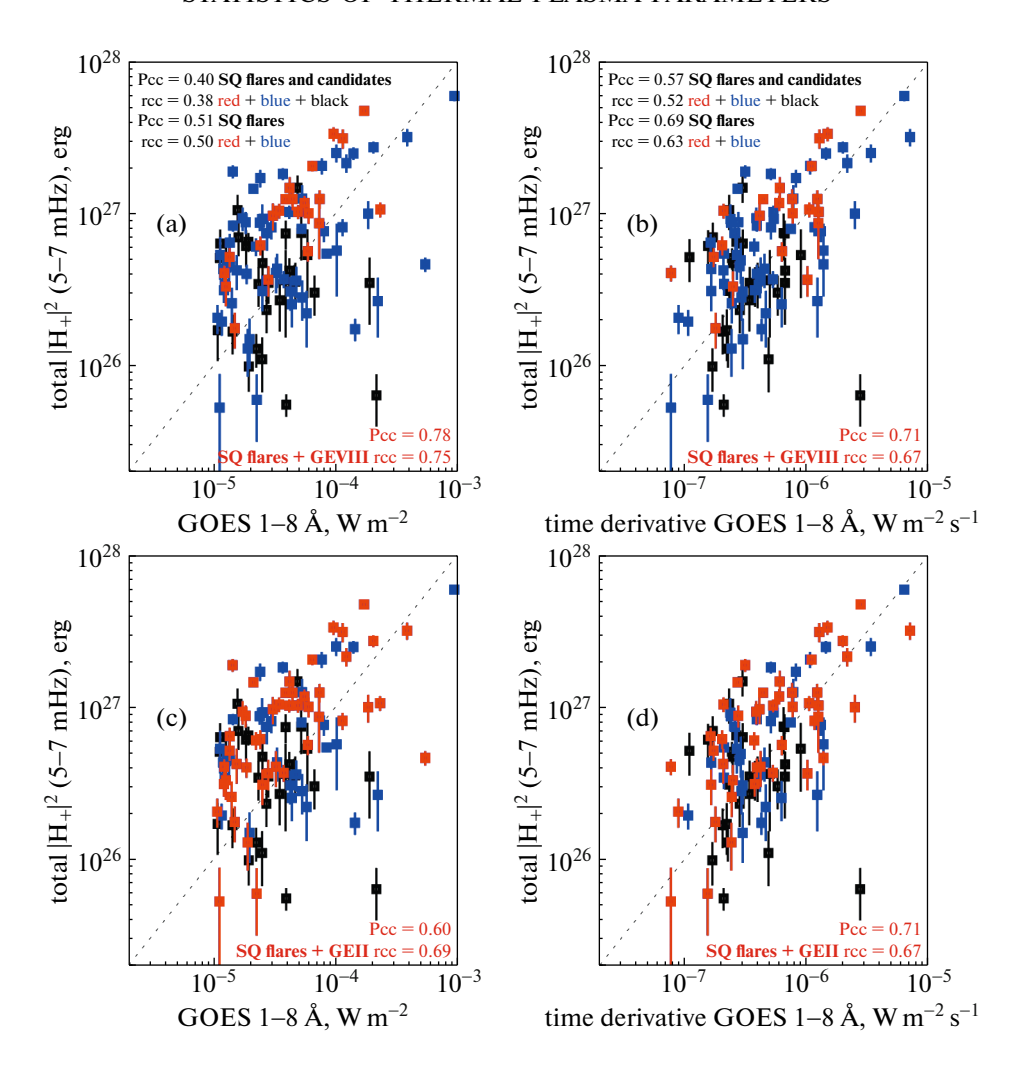


Fig. 1. Dependences of the total acoustic power of sunquakes from the SQ24 catalog in the frequency range 5-7 MHz on the GOES flare class (a, c) and the maximum time derivative in the GOES 1-8 Å channel (b, d). Flares with reliable solar quake detections for which the X-ray spectrum in GEVIII was analyzed (denoted as "SQ flares + GEVIII") are shown in red in panels (a) and (b). Sunquake flares for which the DEM was analyzed within the GEII catalog (denoted as "SQ flares + GEVII") are shown in red in panels (c) and (d). Blue color indicates events outside the GEVIII (a and b) and GEII (c and d) catalogs. Flashes shown in black are candidate sunquakes from the SQ24 catalog. The dotted line corresponds to the bisector. Pearson correlation coefficients (Pcc) and rank correlation coefficients (rcc) are shown directly in the panels.

to expand statistics further and will limit ourselves only to "reliable" events.

Next we will discuss the catalogs used with solar flare parameters. First of all, it is worth noting that we decided not to conduct our own global analysis of solar flare parameters due to the extreme complexity of such work. It was decided to use the results of other statistical studies that examined solar flares without reference to helioseismic effects. Today, there are unique catalogs with a large number of parameters of solar flares, determined within the framework of the Global Energetics of Solar Flares project, presented in a series of 12 articles published from 2014 to 2020 by Markus Aschwanden. These works examined a variety of aspects of the energy release of solar flares of the 24th cycle of solar activity in the date range

January 1, 2010—January 31, 2014: parameters of thermal plasma, characteristics of accelerated electrons, CME dynamics, magnetic energies, etc. All tables from these works were published on the Internet on the VizieR On-line Data Catalog website. In our work, we will touch only two articles that describe the analysis of the parameters of thermal and non-thermal X-ray spectra [41] (hereinafter referred to as the GEVIII catalog, see https://cdsarc.cds.unistra.fr/viz-bin/cat/J/ApJ/881/1) and characteristics of thermal plasma obtained using DEM analysis [42] (hereinafter referred to as the GEII catalog, see https://cdsarc.cds.unistra.fr/viz-bin/cat/J/ApJ/802/53).

In Fig. 1, we highlight in red those flares from the SQ24 catalog for which the X-ray spectra were analyzed (22 flares in total) within the framework of work

[41], on which the GEVIII catalog was compiled. It is noteworthy that for this limited sample the correlation coefficient is 0.78 according to Pearson in Fig. 1a (versus 0.71 for panel (b), where along the x-axis we consider the GOES class. These values are not consistent with the results of the analysis of the entire sample from SQ24: for the entire set of blue and red dots, we have a Pearson correlation coefficient of 0.51 (Fig. 1a) and 0.69 (Fig. 1b). Most likely, this discrepancy is due precisely to the small sample size. In a sample of 22 events, it is not possible to say exactly how much one correlation is better than another. A comparison of 0.71 and 0.78 indicates that both correlations are quite good, considering the correlation coefficient error (standard deviation): ± 0.16 and ± 0.14 . Further statistical analysis of flare parameters will clarify the real relationships. In the case of flares for which DEM analysis was carried out (GEII catalog), we have a sample of 46 events. In this case, comparison of correlations for similar dependencies in Figs. 1c, 1d do not show significant discrepancies with the results of [29]: 0.6 ± 0.11 for the GOES class and 0.71 ± 0.12 for the time derivative.

In the section in which we will consider the correlation dependences of sunguake energy on various parameters, we will evaluate the reliability of the correlation using the t-test with a confidence threshold of 95 percent. If the criterion is met, we will call the correlation satisfactory. For confidence thresholds of 99 and 99.9%, the correlation will be called good and excellent, respectively. When comparing the normalized distributions of parameters of two groups of flares (with sunguakes and without photospheric disturbances), we will use the Mann-Whitney U test (comparison of distribution medians, function "rs test.pro" in IDL) and the Kolmogorov-Smirnov test (procedure "kstwo.pro" in IDL) with a probability threshold of 5%. In other words, different distributions will have lower probabilities of matching the distributions and their medians. Moreover, it will also be important to compare the absolute values of the medians. The criteria may indicate differences in distributions, but the medians will differ very little and there will be no obvious physical meaning in the difference between the distributions. From our subjective point of view, a difference in medians of approximately three times gives the minimum threshold at which we will talk about the difference between distributions on average. If we have a number of five and even an order of magnitude, then we are talking about a clear difference between the distributions on average. Of course. the criteria used should give low probabilities. It is especially important when comparing distributions to identify those parameters for which we have the greatest difference.

Later in the text, we will discuss some details of the methods for calculating flare parameters for the GEII and GEVIII catalogs. Next, the next three sections will be devoted to specific problems of statistical anal-

ysis: analysis of thermal plasma parameters from RHESSI X-ray spectra, statistics of parameters from non-thermal X-ray spectra from RHESSI, analysis of thermal plasma parameters from DEM analysis obtained using AIA ultraviolet images.

3. STATISTICS OF THERMAL PLASMA PARAMETERS ACCORDING TO X-RAY SPECTROSCOPY DATA

Comparing the GEVIII and SQ24 catalogs, we find 22 flares in which X-ray spectra were studied for energies above 3 keV (spectrum analysis boundaries are floating) over the duration of the entire event. It is worth noting that we use tables from the article [41], although the article [43] was previously published, which also considers the analysis of thermal plasma and non-thermal energy of accelerated electrons using RHESSI data. Our choice in favor of a later catalog is dictated by the fact that the catalog based on the first work in 2016 shows the parameters of X-ray spectra only from the position of the "warm target" model [44], in which the low-energy boundary of the spectrum of accelerated electrons determined by the plasma temperature and power index. The later GEVIII catalog is an expansion of the 2016 version using different models of the low-energy edge of the accelerated electron spectrum. In this section we will not talk about the problem of the low-energy boundary (see the next section), since here we will only discuss the parameters of the thermal X-ray spectrum: maximum temperature, emission measure and thermal energy of the plasma. These parameters, as well as estimates of the characteristic linear dimensions of the flare region and flare duration, are available on the Internet only for the GEVIII catalog.

Figure 2 compares the normalized distributions (histograms) of various flare parameters for two samples: 22 flares with a helioseismic response (red) and 72 flares without photospheric disturbances (black). For comparison, we also indicate the values of the medians of the distributions and the ratio of the two medians. The greatest differences in medians are characteristic of the distributions of the maximum emission measure EM (Fig. 2a), the estimate of the thermal plasma density $n_{\rm th} = \sqrt{EM/L^3}$ (Fig. 2e) and the maximum thermal energy $E_{\rm th} = 3k_{\rm B}T\sqrt{EM/L^3}$ (Fig. 2d), where L is the characteristic linear scale of the flare region. Also, what is most striking about these distributions is their relative shift, both "in general" and in terms of the position of the distribution maximum.

For the two samples considered, the distributions of linear scales (Fig. 2c), maximum temperatures (Fig. 2b) and characteristic durations of flares (Fig. 2f) are almost identical in terms of the shape of the distribution, the position of maxima and medians. An esti-

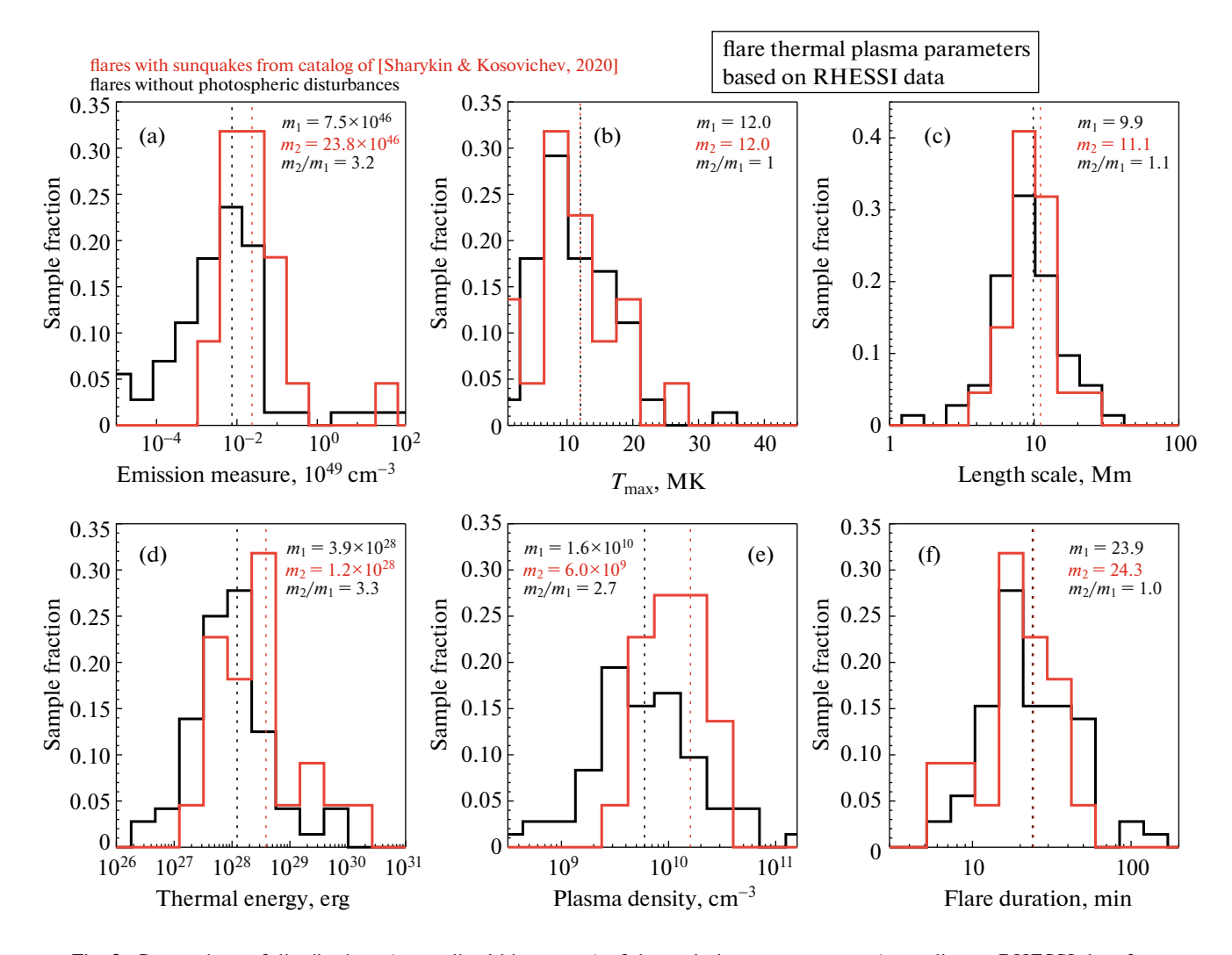


Fig. 2. Comparison of distributions (normalized histograms) of thermal plasma parameters (according to RHESSI data from GEVIII): (a) emission measure, (b) peak temperature, (c) characteristic linear scale, (d) thermal energy, (e) plasma concentration, (f) flare duration according to RHESSI catalog. Histograms are shown for a group of flares with a helioseismic response (red) and without it (black). Vertical lines show median values, which are also duplicated by numbers in the panels of the figure.

mate of the characteristic length scale of the flare region is the result of an analysis of DEM maps (more details in [45]), in which regions above a certain fixed value of the emission measure were identified. The durations of flares in GEVIII were taken from the GOES catalog as the difference between the time of the end of the event and its beginning.

It is worth paying special attention to the identity of the distributions of characteristic flare durations. The thing is that this fact contradicts the conclusions of work [29], which examined the temporal characteristics of flares with sunquakes on the GOES database and showed that flares with sunquakes are on average shorter in duration compared to flares without a photospheric response. However, in [29], the durations of the pulse phases were determined from the curve of the derivative of the soft X-ray flux in the 1–8 Å channel (the time interval during which the derivative of

the flux is above 0.1 from its maximum). We noticed that when using the start time according to GOES data, the flare durations do not differ so much (Fig. 2f) in the two samples, since the algorithm for fixing the start of a flare often works at low radiation fluxes in the pre-flare phase. Whereas the conditional end of a flare is determined by the time the flux decreases by half compared to the maximum (determined reliably due to high flux values). Also, the coincidence of the distribution of flare durations in this study may be associated with the following type of selection effect. RHESSI observes the Sun at periodic intervals associated with entry into the Earth's shadow and sometimes into the southern magnetic anomaly (detectors are oversaturated due to high radiation fluxes). On average, there is about 40-50 minutes of observation time per revolution. This is most likely why flashes with times less than 60 minutes were selected (being

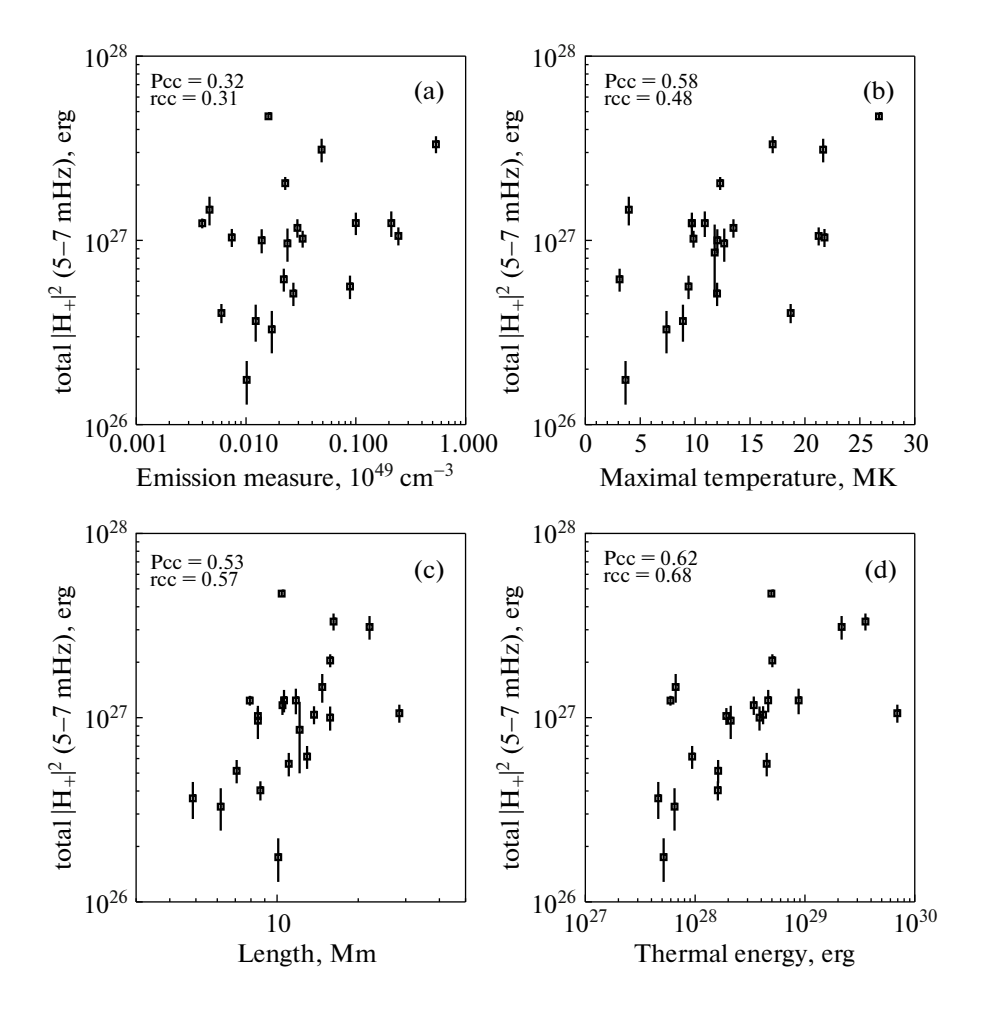


Fig. 3. Dependences of the total acoustic power of sunquakes for 22 flares in the frequency range 5–7 MHz on thermal plasma parameters (according to RHESSI data from GEVIII): (a) emission measure, (b) peak temperature, (c) characteristic linear size, (d) thermal energy. The Pearson correlation coefficient (Pcc) and rank correlation coefficient (rcc) values are indicated in the panels of the figure.

more likely to be fully observed). For longer flares, the probability of measuring their full duration is lower. We believe that the discrepancy under discussion is an artifact of the GEVIII catalog compilation methodology and the peculiarities of observations of the Sun by the RHESSI and GOES spacecraft. Thus, from our point of view, the result about the pronounced pulse of helioseismically active flares is not canceled.

In Fig. 3, we present an analysis of the dependences of the parameters of helioseismically active flares from the GEVIII catalog on the total energy of the sunquake in the frequency range 5–7 MHz. The figure shows the values of the Pearson correlation coefficient ($P_{\rm cc}$) and the rank correlation coefficient ($r_{\rm cc}$). In what follows, for brevity, we will only mention the Pearson correlation. It can be seen that for thermal energy (Fig. 3d) we have the correlation $P_{\rm cc} = 0.62$ (the best of all thermal parameters) with solar earthquake energy, despite the lack of a linear relationship with the emission measure ($P_{\rm cc} = 0.32$). This fact, in particular, is

due to the fact that the correlation of helioseismic energy with temperature (Fig. 3b) and characteristic size (Fig. 3c) is 0.58 and 0.53, respectively. It can be seen that these values differ greatly from the correlation $P_{\rm cc}=0.78$ for the GOES class (Figs. 1a–1b), which again indicates a small number of events in the sample of flares with sunquakes. We will check these dependencies below using DEM data, for which the sample is approximately twice as large.

To summarize this section of the article, we will highlight and repeat the statistical results obtained. Firstly, a comparative analysis of the thermal plasma parameters (according to RHESSI data) of flares without photospheric disturbances with the same parameters of helioseismically active flares shows:

(1) the presence of small differences in the distribution of parameters for the two samples. There are slight shifts in the distributions relative to each other, showing that flares with sunquakes, on average, emit a little more due to a larger emission measure (medians 23.8×10^{46} and 7.5×10^{46} cm⁻³), have a slightly higher plasma density (1.6 × 10¹⁰ and 6.0 × 10⁹ cm⁻³), and also have a higher maximum thermal plasma energy (3.9 × 10²⁸ and 1.2 × 10²⁸ erg);

- (2) distributions of temperature (median 12 MK for both distributions), characteristic sizes of the flare region (11.1 and 9.9 Mm) and flare duration (24.3 and 23.9 min) for these two samples practically do not differ from each other:
- (3) the identity of the duration distributions is most likely a feature of the GOES flare recording method and the RHESSI observation conditions. This fact does not contradict a more accurate analysis in article [29], which showed that flares with sunquakes are more impulsive and shorter in duration compared to flares without a photospheric response.

Secondly, studies of the relationships between the power of helioseismic disturbances and thermal plasma parameters have revealed the following features:

- (1) the more powerful the helioseismic flare, the larger it is in size, the hotter it is and the more total thermal plasma energy it has. For these dependencies, the correlation coefficients are in the range of 0.53–0.62;
- (2) the energy of sunquakes does not have a linear relationship with the measure of plasma emission ($P_{cc} = 0.32$).

4. STATISTICS OF NON-THERMAL X-RAY SPECTRUM PARAMETERS

In this section, we will discuss the statistical analysis of parameters of the non-thermal X-ray spectrum using the GEVIII catalog. The number of flares without photospheric disturbances and events with helioseismic activity is the same as in the previous section, where thermal plasma parameters were considered. We will first perform a comparative analysis of the two samples, and then conduct a correlation analysis between the parameters of the non-thermal X-ray spectrum, the non-thermal energy of accelerated electrons and the energy of sunquakes.

For the physics of solar flares, one of the central problems in determining the integral characteristics of accelerated electrons (flux, density, energy) is determining the value of the low-energy boundary in the spectrum, which is determined by the physics of the acceleration process. It is often fixed at some standard value (for example, 20 keV). It is also sometimes possible to determine the value of the low-energy boundary when approximating the spectrum of hard X-ray radiation within the framework of an optimization algorithm for fitting the model to real data. Some analytical models allow one to estimate the value of the low-energy boundary based on physical assumptions. In particular, within the framework of the warm target model [44], the low-energy boundary is determined by the plasma temperature and the power-law index of the spectrum of accelerated electrons. The value of this energy boundary can be several times less than the typical value of the intersection of the thermal and power parts of the X-ray spectrum (~20 keV). In [43], the low-energy limit and the value of the total nonthermal energy of accelerated electrons were given only within the framework of the warm target model. We are interested in data not only on non-thermal energy, but also the main parameters of the non-thermal spectrum: the normalization factor for an energy of 50 keV (which determines the X-ray flux density at a given energy), the power index of the non-thermal X-ray spectrum, the low-energy boundary (the intersection of the thermal and non-thermal parts of the spectrum). Based on these parameters of the nonthermal X-ray spectrum, this section analyzes the results of a statistical study.

The choice of parameters for statistical analysis was dictated by the following considerations. The fact is that, based on the basic parameters of the photon spectrum, we can determine the characteristics of the spectrum of accelerated electrons, which is also power law. Then, using one or another physical model (including the warm target model), one can estimate the total energy and flux of accelerated electrons. We will use the classical "thick target" model [34], in which the low-energy boundary is one of the parameters. Note that any statistical study involves constructing dependencies (histograms) of the number of events on a number of parameters that follow from observations or are obtained under simplifying assumptions (models). In our case, we will carry out a statistical study of the distribution of the number of flares, first of all, for the parameters of the X-ray spectrum, from which we can indirectly judge the characteristics of accelerated electrons by considering the "thick target" model. For this kind of statistical research, the use of more complex models of the interaction of accelerated electron beams in the magnetically active plasma of flare loops seems premature.

A comparison of the distributions of parameters of the non-thermal X-ray spectrum for two samples of flares is shown in Fig. 4. In contrast to the distributions of thermal parameters (described in the previous section), here we observe a strong separation of the histograms. The most striking difference between flares with sunquakes and flares without photospheric disturbances is when comparing the distributions of the normalization coefficient of the power-law spectrum (Fig. 4a). The difference in medians reaches 16.7 times in favor of the sample of helioseismically active flares. Note that this difference is determined by the narrow half-width of the distributions, which is approximately an order of magnitude of the parameter. These distributions are clearly separated and practically do not intersect due to their narrowness. If we compare the peaks of the probability distributions, the difference is slightly smaller and is approximately an order of magnitude.

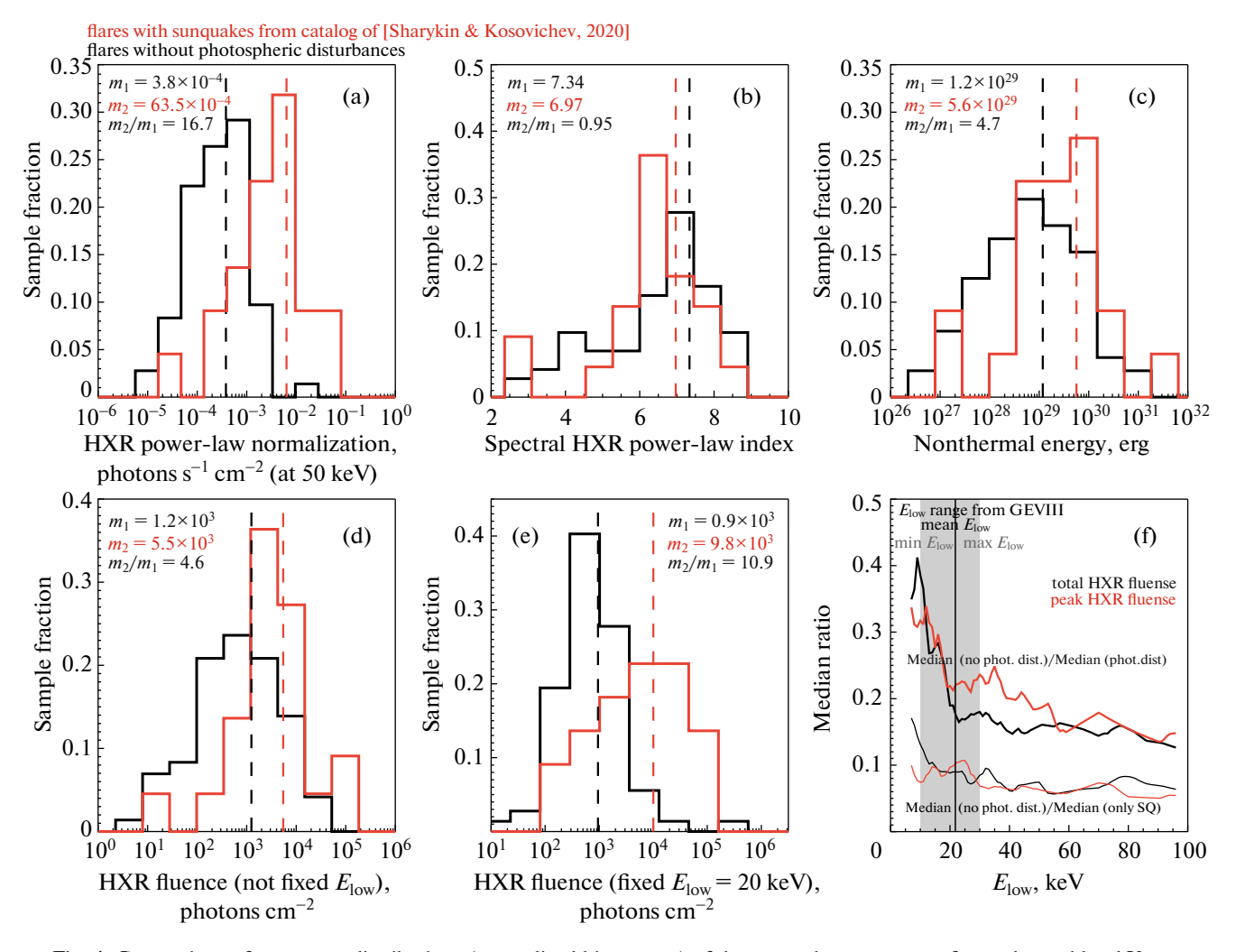


Fig. 4. Comparison of parameter distributions (normalized histograms) of the power-law spectrum of non-thermal hard X-ray radiation (according to RHESSI data from GEVIII). Vertical dashed lines show median values, which are also duplicated by numbers in the panels of the figure. Histograms are shown for a group of flares with a helioseismic response (red) and without it (black). Panel (f) shows the behavior of the ratio of median values as a function of the value of the low-energy cutoff (above which the X-ray spectrum is integrated) for two distributions of non-thermal X-ray spectrum parameters: the total X-ray flux over the entire duration of the flare (black) and at its peak (red). The median ratios are calculated for two pairs of flare samples: for flares with sunquakes and without photospheric disturbances (thin lower lines), for flares with and without photospheric disturbances (thick upper lines). The vertical gray bar shows the range of low energy boundaries from minimum to maximum values. The vertical black line corresponds to the average value of the distribution of low-energy boundaries.

Another important result is related to the comparison of the distributions of power-law indices of non-thermal X-ray spectra (Fig. 4b). The analysis showed that the histograms differ slightly from each other. In both distributions, the median value is approximately 7: 7.3 for flares without photospheric disturbances and 7.0 for flares with sunquakes.

In terms of non-thermal energies (Fig. 4c), the distributions differ in medians by a factor of approximately five. The values of non-thermal energies were calculated within the framework of the "thick target" model. To calculate the total non-thermal energy, we integrated the spectrum of accelerated electrons above the energy value (low-energy boundary) corresponding to the intersection of the power-law part of the

X-ray spectrum with its thermal part. In this article, we do not compare the distributions of the low-energy boundaries themselves due to the layout of the figure. We will only point out that these distributions are very similar to each other, and also show the average, minimum and maximum values of the low-energy edges in Fig. 4f with a gray bar and a black line (average value). Note that here the difference between the histogram medians is not so significant (about 5 times) compared to the case of distributions depending on the normalization coefficient. Also, the histograms have a wider shape, which is most likely due to the greater uncertainty of the low-energy boundary (further $E_{\rm low}$). Later in the text we present a parametric analysis considering different values of the low-energy cutoff,

above which we integrate the spectrum of X-ray photons. If we consider the fluxes of accelerated electrons [electrons s⁻¹] (approximately equal to the quotient of non-thermal energy and low-energy boundary), we obtain distributions similar to the distributions of non-thermal energies in Fig. 4c.

In Figs. 4d and 4e we compare the distributions of the calculated integral hard X-ray flux above the lowenergy boundary determined from the intersection of the thermal and non-thermal components of the X-ray spectrum (panel 4d) and for a fixed lower energy value of 20 keV (panel 4e) for the duration of the entire flare. Assuming that the real dynamic spectrum of non-thermal X-ray photons is a power-law in energy and time $I(E,t) = A_{50}(t)(E/50)^{-\gamma(t)}$, where A_{50} is the normalization coefficient of the X-ray spectrum at an energy of 50 keV, and γ is the power-law index of the X-ray spectrum, we obtain an estimate of the total flux based on the available values of the GEVIII catalog as follows:

$$I_{\text{tot}} = \int_{t_{\text{start}}}^{t_{\text{fin}}} \int_{l_{\text{low}}(t)}^{\infty} I(E, t) dE dt$$

$$\sim A_{50} \left(\frac{E_{\text{low}}}{50 \text{ keV}}\right)^{-\gamma} \frac{E_{\text{low}}}{\gamma - 1} \tau_{\text{flare}}.$$
(1)

Here, we made a transition through the "~" sign from real values, time-varying parameters of the non-thermal X-ray spectrum, to fixed values from the GEVIII catalog, which do not reflect the dynamics of the spectrum in any way. The quantity τ_{flare} corresponds to the characteristic duration of the flare, which re-evaluates the time of the pulse phase with hard X-ray radiation. In fact, the presented expression is an upper estimate of the total photon flux [photons cm⁻²]. If we discard integration over time, we obtain an estimate of the maximum during the flare of the flux of X-ray photons [photons s⁻¹ cm⁻²].

Comparison of histograms in Figs. 4d and 4e shows the distributions of the integral flux of liquid radiation shifted relative to each other for the two classes of flares under consideration. The group of flares with solar quakes is particularly strikingly different from the flares without photospheric disturbances in Fig. 4e, where we consider a fixed low-energy cutoff value of 20 keV (roughly the average of the distribution of all flares from GEVIII). Here, the medians differ by an order of magnitude, and the maxima of the distributions are even greater, while for the unfixed lowenergy boundary taken from the catalog, the medians differ by about a factor of five. Generally speaking, the difference in the medians of the distributions under consideration indicates significant differences (between two samples) for all integral characteristics of accelerated electrons, since the formulas for determining these characteristics (see [34]) include the integral photon flux. Note also that the difference in the distributions of non-thermal photon fluxes and the normalization coefficient is greater (the difference in the medians is an order of magnitude) than in the case of thermal parameters (the medians differ by a maximum of three times), discussed in the previous section. This indicates the fundamental importance of accelerated particles for the helioseismic activity of flares and provides a compelling additional argument in favor of the model of sunquakes generation by beams of accelerated particles injected into the dense layers of the solar atmosphere.

The last panel of Fig. 4 shows the results of a parametric analysis of the ratio of the median distributions of the total photon flux (black) for the entire flare and the maximum flux during the flare (red) depending on the value of the low-energy boundary (on the x-axis from 7 to 90 keV). Moreover, we consider two different pairs of distributions in order to emphasize the difference between flares with photospheric disturbance and without photospheric response. The first pair corresponds to what we considered in all previous panels of Fig. 4 and in all histograms in Fig. 2: comparison of flares without photospheric disturbances and helioseismically active flares, i.e., those events that gave rise to the sunquake (thin lower lines). The second pair of distributions compares flares with and without photospheric disturbances (thick top lines). Let us recall that not all flares with photospheric disturbances recorded on Dopplerograms or HMI continuum maps are characterized by the presence of helioseismic waves. Thus, we additionally consider the more general case of flares with photospheric activity, which include a subset of helioseismically active flares (41 flares in the sample).

Figure 4f shows that for a wide range of values of the low-energy cutoff we have a significant difference in the distributions of flares with solar quakes and flares without photospheric disturbances. This difference is about an order of magnitude throughout the entire considered range of low-energy boundary values. In the case of the second pair of distributions (flares with and without photospheric disturbances), this difference is approximately five times (for energies above approximately 20 keV) in favor of flares with photospheric disturbances. For lower energies the difference begins to decrease. As a result, we see that photospheric disturbances in the general case (including without sunguakes) and sunguakes in particular (and to a greater extent) are clearly associated with increased fluxes of accelerated electrons compared to flares without any photospheric manifestations.

Figure 5 shows the results of an analysis of the dependences of helioseismic power on the parameters of the non-thermal X-ray spectrum, which we discussed above in the case of histograms in Fig. 4. For the normalization coefficient for the energy of 50 keV and the duration of the flare, we have, respectively, a correlation with the coefficients: 0.56 and 0.51

(Figs. 4a and 4c). In the case of the power index, there is no correlation ($P_{cc} = 0.18$).

Figures 5d-5f show the dependences of the total acoustic power of sunquakes for 22 flares in the frequency range 5-7 MHz on the parameters of the nonthermal X-ray spectrum—the integral flux of X-ray radiation for the duration of the entire flare, the maximum flux and the total non-thermal energy of accelerated electrons for the entire flare time within the framework of the "thick target" model. In black, we denote the case of an unfixed low-energy edge of the spectrum of accelerated electrons, which we took from the GEVIII catalog. The highest value of the correlation coefficient is 0.61 for the total X-ray flux over the entire duration of the flare (Fig. 5d). The non-thermal energy of accelerated electrons correlates least of all with the energy of sunquakes ($P_{cc} = 0.51$). The calculation results for a fixed low-energy boundary of 20 keV are indicated in red. Note that in this case the correlation coefficient becomes higher: in Figs. 5d and 5e the correlation coefficient takes the value of 0.68 (confidence probability more than 99.9%), and for non-thermal energy in Fig. 5f, it increases to 0.55.

Comparison of histograms and the results of correlation analysis for the case of a floating value of the energy of the normalization factor shows results similar to those shown in Fig. 4f and Figs. 5g-5i. If the analysis is carried out for higher energies (both for normalization and for the low-energy boundary), for example, up to 300 keV (as in [Wu2023]), then we obtain a weak correlation between the integral flux of non-thermal X-ray photons and the energy of sunquakes, which most likely follows from the uncertainty of the type of energy spectrum in the region above 100 keV—the spectrum may differ in slope and have, for example, a break. Therefore, we consider lower bounds on the energy and normalization of the spectrum to an energy of 100 keV and continue the spectrum model-wise with one power.

An analysis of the dependence of the correlation coefficient on the value of the fixed low-energy boundary for plots of type 5d-5f is shown in panels 5g-5i. The range of variation of the low-energy boundary is similar to the case in Fig. 4f and is 7–90 keV. The graphs show dependencies for both the rank correlation coefficient and the Pearson coefficient (a smoother curve). The gray stripe shows the boundaries from the minimum to the maximum value of the low-energy boundary from the sample from the GEVIII catalog. The vertical line shows the average value of the low-energy boundary for this sample. Note that for the total flux (Fig. 5g) and the maximum flux (Fig. 5h) of X-ray radiation, the correlation coefficient peaks at 20 keV for the Pearson coefficient and at 15 keV for the rank correlation coefficient. For higher energies, the relationship between the characteristics under consideration and the energy of sunquakes begins to deteriorate. This fact indicates a possible weak relationship between sunquakes and the high-energy part of the spectrum of accelerated electrons. For the non-thermal energy of accelerated electrons (Fig. 5i), the Pearson correlation coefficient peaks (has a very flat shape) around 30 keV and for the rank correlation coefficient the maximum is reached at the low-energy edge of about 25 keV. Moreover, the correlation is generally worse compared to the correlation shown in the graphs in Figs. 5g and 5h.

Let us summarize the statistical results obtained above. First, a comparative analysis of the parameters of the non-thermal X-ray spectrum (according to RHESSI data) of flares without photospheric disturbances with the same parameters of helioseismically active flares shows:

- (1) the sample data differ most in the distribution of the normalization coefficient of the power-law non-thermal X-ray spectrum for an energy of 50 keV. The ratio of the medians of the two distributions is almost 17 in favor of flares with sunquakes;
- (2) when comparing the distributions of total (over the entire duration of the flare) and maximum fluxes of non-thermal X-ray radiation, we also discovered a significant shift in the distributions relative to each other. The ratio of the distribution medians becomes even larger (roughly an order of magnitude) when considering fixed values of the low-energy cutoff above which we integrate the spectrum. An analysis of the dependence of the ratio of medians on the choice of the value of the low-energy boundary showed that for a wide variety of values, the difference in medians varies slightly and is approximately an order of magnitude;
- (3) for the distributions of non-thermal energy of accelerated electrons within the framework of the "thick target" model, a difference in distributions was also established. The ratio of medians is approximately 5 times;
- (4) analysis of the distributions of power indices of the non-thermal X-ray spectrum showed a slight difference between these samples.

Secondly, the analysis of correlations between the power of helioseismic disturbances and the parameters of non-thermal X-ray spectra revealed the following features:

- (1) a complete lack of correlation between the energy of helioseismic disturbances and the power-law index of the non-thermal X-ray spectrum was discovered;
- (2) a correlation ($P_{\rm cc}=0.61$) was found between helioseismic energy and the total flux of non-thermal X-ray radiation for the entire flare in the case of an unfixed value of the low-energy boundary (taken from the GEVIII catalog). For a fixed low-energy boundary $E_{\rm low}=20$ keV, the maximum value of the correlation coefficient is 0.68;

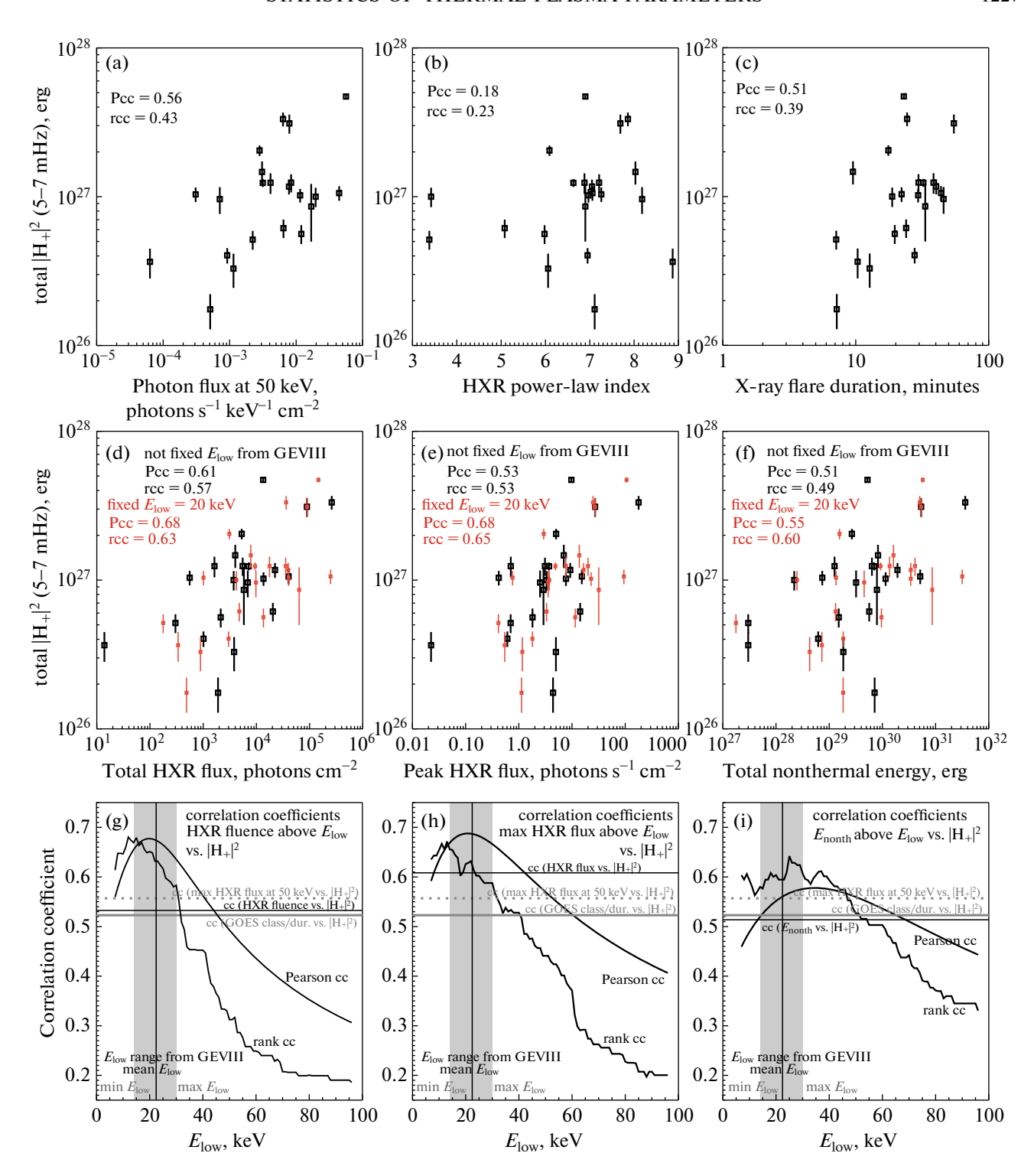


Fig. 5. Dependences of the total acoustic power of sunquakes for 22 flares in the frequency range 5–7 MHz on the parameters of the non-thermal X-ray spectrum (according to RHESSI data from GEVIII). Figs. 5d–5f show in black the dependences in the case of integrating the spectrum above the low-energy cutoff taken from GEVIII (the value of this cutoff is not fixed). Red color indicates the case of using a fixed low-energy cutoff value of 20 keV for all events. The Pearson correlation coefficient (Pcc) and rank correlation coefficient (rcc) values are indicated in the panels of the figure. Figs. 5g–5i examine the dependence of the correlation coefficient (rank and Pearson) on the value of the low-energy cutoff above which we integrate the spectrum. The analysis is carried out for X-ray spectrum parameters similar to Figs. 5d–5f. Horizontal lines correspond to the values of correlation coefficients for different parameters indicated in the text in the figure. The vertical gray bar shows the range of low energy boundaries from minimum to maximum values. The vertical black line corresponds to the average of the distribution of low-energy boundaries from GEVIII.

(3) the correlation coefficient between helioseismic energy and the total non-thermal energy of accelerated electrons for the entire duration of the flare is 0.58, if we consider the fixed $E_{\text{low}} = 30$ keV. For unfixed values $P_{\text{cc}} = 0.51$.

Generally speaking, all the results can be reduced to one conclusion—helioseismically active solar flares are events that are more saturated with accelerated electrons compared to flares without photospheric disturbances. This conclusion is an additional strong argument in favor of the main hypothesis about the causes of sunquakes associated with the penetration of non-thermal electrons into the lower layers of the solar atmosphere.

5. STATISTICS OF THERMAL PLASMA PARAMETERS OBTAINED FROM ANALYSIS OF THE DIFFERENTIAL EMISSION MEASURE

In the previous two sections, we examined the statistics of solar flares based on observations of X-ray radiation by the RHESSI space observatory. In particular, we studied the features of solar flares with a helioseismic response from the point of view of the thermodynamic parameters of hot plasma—the maximum values of the emission measure, temperature and thermal energy. The obtained statistics indicate the presence of a correlation between the sunquake energy and the maximum thermal energy ($P_{cc} = 0.62$) and temperature ($P_{cc} = 0.58$) of the heated plasma. It turned out that the correlation with the emission measure is not high ($P_{cc} = 0.32$). In this section, we present the results of a statistical analysis of the thermodynamic parameters of flares for extended samples based on observations of extreme ultraviolet (EUV) radiation from AIA/SDO data, which allow us to complement the obtained results on the distributions of thermodynamic parameters of flares from RHESSI data. Statistical analysis is also divided into two parts: (1) comparative analysis of the distributions of parameters of flares with sunguakes and flares without sunquakes; (2) correlation analysis of the relationships between the thermodynamic parameters of flare plasma and the energy of sunquakes calculated by the acoustic holography method.

Next, we provide a relatively brief description of the AIA ultraviolet space telescope and the technique for analyzing plasma heating using the DEM forward-fitting method [45], which formed the basis of the GEII catalog [42]. Despite the detailed description in the original article, we must point out the main features of the method in order to further understand the difference with X-ray spectroscopy within the scope of this article.

The AIA telescope [40] on board SDO [31] carries out spatially resolved observations of EUV radiation in a wide range of wavelengths in seven channels: 94

(Fe XVIII, 7.2 MK), 131 (Fe VIII and XXI, 0.5 MK), 171 (Fe IX, 0.8 MK), 193 (Fe XII and XXIV, 1.5 MK), 211 (Fe XIV, 1.9 MK), 304 (He II, 0.08 MK) and 335 Å (Fe XVI, 2.5 MK). This set of channels allows one to study the temperature structure of the corona in a wide range from 0.06 to 20 MK. Using EUV maps of flare regions [42], a GEII catalog of thermodynamic parameters of M and X flares was compiled, determined by analyzing the DEM of flare plasma. This approach involves determining the function $DEM(T) = n_e^2 dz/dT$ [cm⁻⁵ K⁻¹] of plasma distribution along the line of sight (coordinate z) depending on temperature T. Note that the analysis of the RHESSI data (for the GEVIII catalog) was carried out within the framework of a single-temperature approximation: the X-ray spectrum (up to approximately 20 keV) was approximated by the model spectrum of bremsstrahlung thermal radiation of an isothermal plasma. The description within the DEM is more complete. Therefore, in addition to checking previous results for RHESSI, we will receive more advanced statistical data.

When determining the emission measure and plasma temperature in the flare region, the authors of GEII used the following technique. At the input there was a data set of dimensions (X, Y, λ, t) , consisting of a time sequence of EUV images: two image coordinates, wavelength of the AIA channel (6 in total minus 304 Å, corresponding to the chromosphere and transition zone), time (with duty cycle 12 s). For each pixel of the EUV map at any time, the DEM was selected in the form of a Gaussian with three variable parameters (peak, temperature of the center of the Gaussian and width) so as to get as close as possible to the intensity values in all 6 channels. Then a contour (determining the size of the flare region) was selected based on some empirically selected value of the Gaussian maximum. The next step was the summation of all Gaussians within the selected contour. Thus, we obtained the spatially integrated DEM of the entire flare region as a function of time. Then, integrating over temperature, we obtain the time dependence of the total emission measure, the maximum value of which is indicated in the GEII catalog.

Temperatures in the GEII catalog are given in two versions. The first value $T_{\rm p}$ corresponds to the maximum peak temperature of the spatially integrated DEM for the entire duration of the flare. The second value $T_{\rm w}$ is the maximum of the average temperature averaged over the DEM. In fact, $T_{\rm w}$ is the center of mass of the DEM and is calculated as follows:

$$T_{\rm w}(t) = \frac{\int T \, DEM(T,t) dT}{\int DEM(T,t) dT} = \frac{\sum_{\rm k} T_{\rm k} DEM(T_{\rm k},t) \Delta T_{\rm k}}{EM(t)}.$$

This formula also shows the transition from continuous to discrete representation. In [42], to determine the DEM, the temperature range of the peaks of individual components of the Gaussians 0.5-30 MK (36 discrete values, equidistant on a logarithmic scale) was considered, while the spatially integrated DEM was determined in an extended temperature range $\lg T_{k} = 5-8$ in order to consider the contribution of the "tails" of the Gaussians for the coldest and hottest DEM components. DEM analysis showed that the values $T_{\rm w} = 6-40$ MK are systematically higher than the values $T_p = 0.5-25$ MK, which means a greater contribution to the total emission measure from plasmas with lower temperatures. In discrete form, the total thermal energy of the plasma in the flare region is calculated using the DEM as follows (for more details, see the Appendix in [42]):

$$E_{\rm th}(t) = 3k_{\rm B}L^{3/2}\sum_{\rm k}T_{\rm k}\left(DEM\left(T_{\rm k},t\right)\Delta T_{\rm k}\right)^{1/2}.$$

For our statistical study, we will use the following information from the GEII catalog: maximum emission measure, characteristic length scale L, $T_{\rm w}$, $T_{\rm p}$, total thermal energy of the plasma, plasma density as $\sqrt{EM/L^3}$.

Figure 6 shows a comparison of the distributions of thermal plasma parameters for a sample of flares with sunquakes and without photospheric disturbances. The most important thing that follows from this figure is the virtually complete identity of the samples: almost identical values of medians, peaks and histogram widths (unlike the RHESSI data in Fig. 2). Thus, when considering the DEM, the difference in distributions previously noted from the RHESSI data disappears. It is necessary to try to understand whether there is physics in this difference. Most likely, this is due to the construction of the DEM, which considers the contribution of plasma with a very wide temperature range.

Correlations of thermal plasma parameters according to DEM and the values of the total energy of helioseismic flare disturbances are shown in Fig. 7. In contrast to the RHESSI data, we have a more obvious dependence of the sunquake energy on the emission measure (Fig. 7a) with a correlation coefficient of 0.56 (about twice as good as in Fig. 3a). The situation with temperatures is the opposite: the correlation is worse for both $T_{\rm w}$ ($P_{\rm cc}=0.43$ versus 0.58 in Fig. 3b) and $T_{\rm p}$ ($P_{\rm cc}=0.36$). The correlation coefficients for the maximum thermal energy of the flare plasma and the characteristic length scale are approximately the same (0.55 and 0.51). It is interesting that for the plasma density determined from DEM there is a weak anticorrelation with the coefficient $P_{\rm cc} = -0.33$. This means that the more a flare manifests itself in helioseismic activity, the more likely it is characterized by a lower plasma concentration. However, the difference in concentrations is very small (10^{11} and 0.8×10^{11} cm⁻³) and the correlation is too small ($P_{\rm cc} = -0.33$) to be confident in this dependence. It is also worth noting that the obtained identical correlations for both types (by RHESSI and by DEM) of maximum thermal energies are the results of the correlation of helioseismic energy with the maximum flare temperature according to RHESSI data in the case of Fig. 3d and correlation with the emission measure determined from DEM (in Fig. 7f).

Also, given the relative narrowness of the distributions of flares by plasma concentrations, as well as the correlation of sunquake energy with the characteristic length scale ($P_{\rm cc}=0.51$ in Fig. 7d), we think that the correlation with the emission measure (Fig. 7a) is more related to the volume of the flare region, because

 $EM = n^2 L^3$. In other words, large sunquakes are associated with the involvement of a larger number of magnetic loops in the flare process. That is, we have an unambiguous "geometric effect of a large flare." At the same time, flares with sunquakes and without photospheric disturbances do not differ in any way in geometric sizes within the framework of the methodology for estimating lengths in the GEII catalog (recall that the lengths in GEVIII are taken from the second GEII catalog).

As a summary of this section, we indicate the following results of statistical analysis of flares based on the DEM of EUV radiation:

- (1) flares with sunquakes and without photospheric disturbances are identical in their distributions of thermodynamic parameters of the flare region within the framework of DEM analysis;
- (2) a correlation ($P_{cc} = 0.56$) was found between the energy of helioseismic disturbances and the emission measure (which differs from the results of the analysis of RHESSI data);
- (3) no correlation was found between the energy of helioseismic disturbances and the temperature estimated from the DEM in two different ways (also contradicts the results of the analysis of RHESSI data);
- (4) we obtained a similar (as for the RHESSI data) correlation between helioseismic energy and the maximum thermal energy of the flare plasma, obtained within the framework of DEM analysis. However, this correlation is more related to the dependence of sunquake energy on the emission measure and the characteristic size of the flare region. Whereas for the RHESSI data we have a linear dependence on temperature and also on length;
- (5) an anti-correlation (the only one in the entire work) was obtained between the energy of sunquakes and the plasma concentration. However, this result has little reliability and in the future it needs to be checked on larger samples or using a more reliable

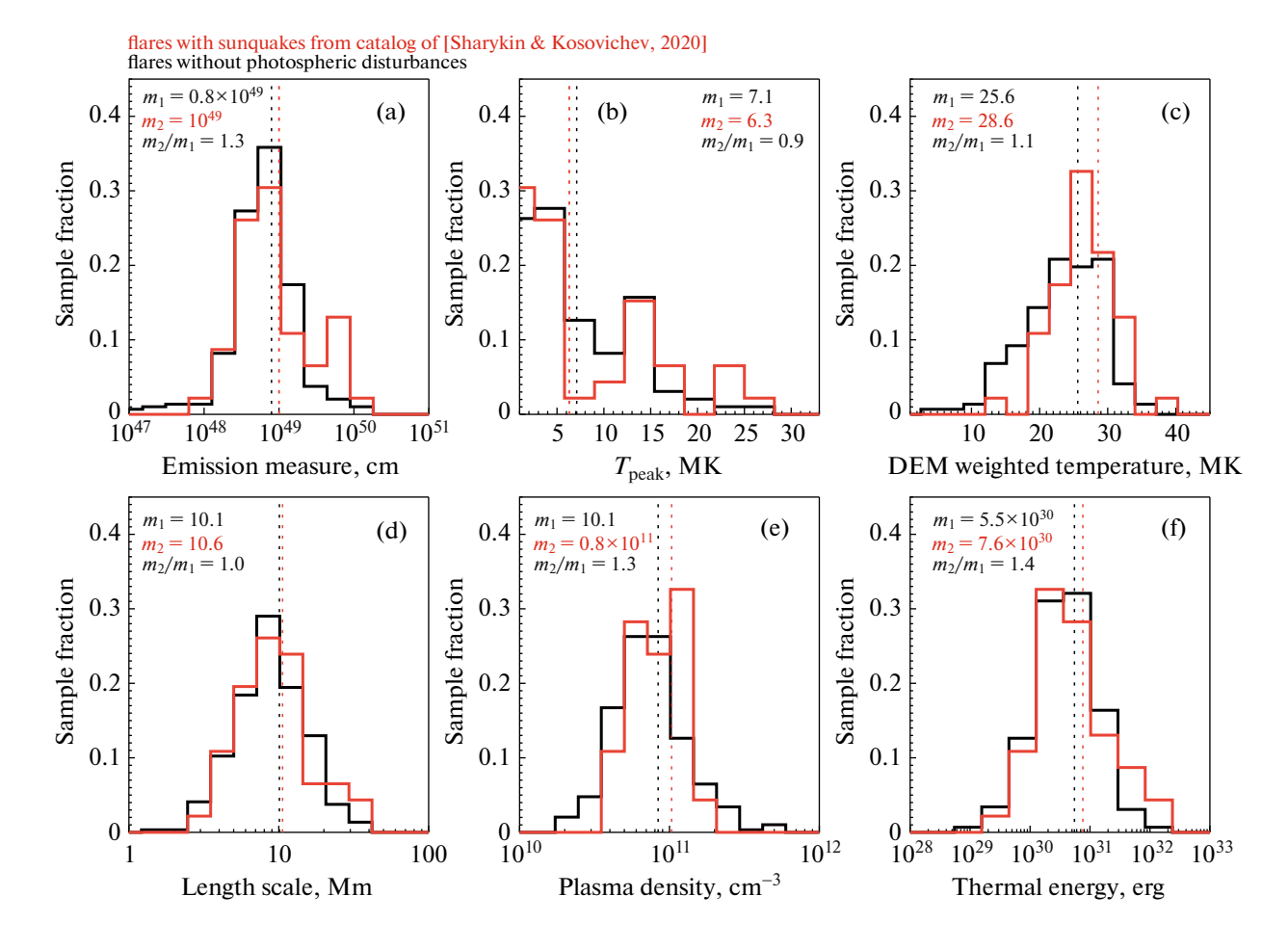


Fig. 6. Comparison of parameter distributions (normalized histograms) of thermal plasma (according to AIA data from GEII): (a) emission measure, (b) LEED peak temperature, (c) LEED-averaged temperature, (d) characteristic linear scale, (e) characteristic concentration plasma, (f) thermal energy. Histograms are shown for a group of flares with a helioseismic response (red) and without it (black). Vertical dotted lines show the median values, which are also duplicated by the numbers m1 and m2 in the panels of the figure.

method for determining the geometric dimensions of flare regions.

6. MAIN RESULTS

As a result of comparing helioseismically active solar flares and flares without photospheric disturbances, we found:

- (1) significant difference in non-thermal X-ray fluxes. On average, the flows of two samples differ by at least an order of magnitude. The maximum ratio (almost 17 times in favor of flares with sunquakes) of the distribution medians was found for the normalization coefficient of the power-law non-thermal X-ray spectrum for an energy of 50 keV;
- (2) we found no differences between the two samples of flares in terms of the distributions of the power-law index of the non-thermal X-ray spectrum (i.e., the hardness of the spectrum of accelerated electrons).

A more important parameter is the integral flux of hard X-ray radiation;

- (3) there is a slight difference in the two considered distributions (bias) of thermodynamic parameters determined from the RHESSI X-ray spectra. Flares with sunquakes have a slightly higher maximum thermal energy, emission measure, and hot plasma concentration (the medians of the distributions differ by about a factor of three);
- (4) comparison of the distributions of characteristic sizes of the flare region showed the identity of two samples of flares within the framework of the technique for identifying the geometric location of a flare using DEM maps;
- (5) it is shown that, from the point of view of DEM analysis, the thermodynamic parameters of the two samples of flares are practically the same.

Analysis of the dependences of helioseismic energy on various parameters of flares obtained in the frame-

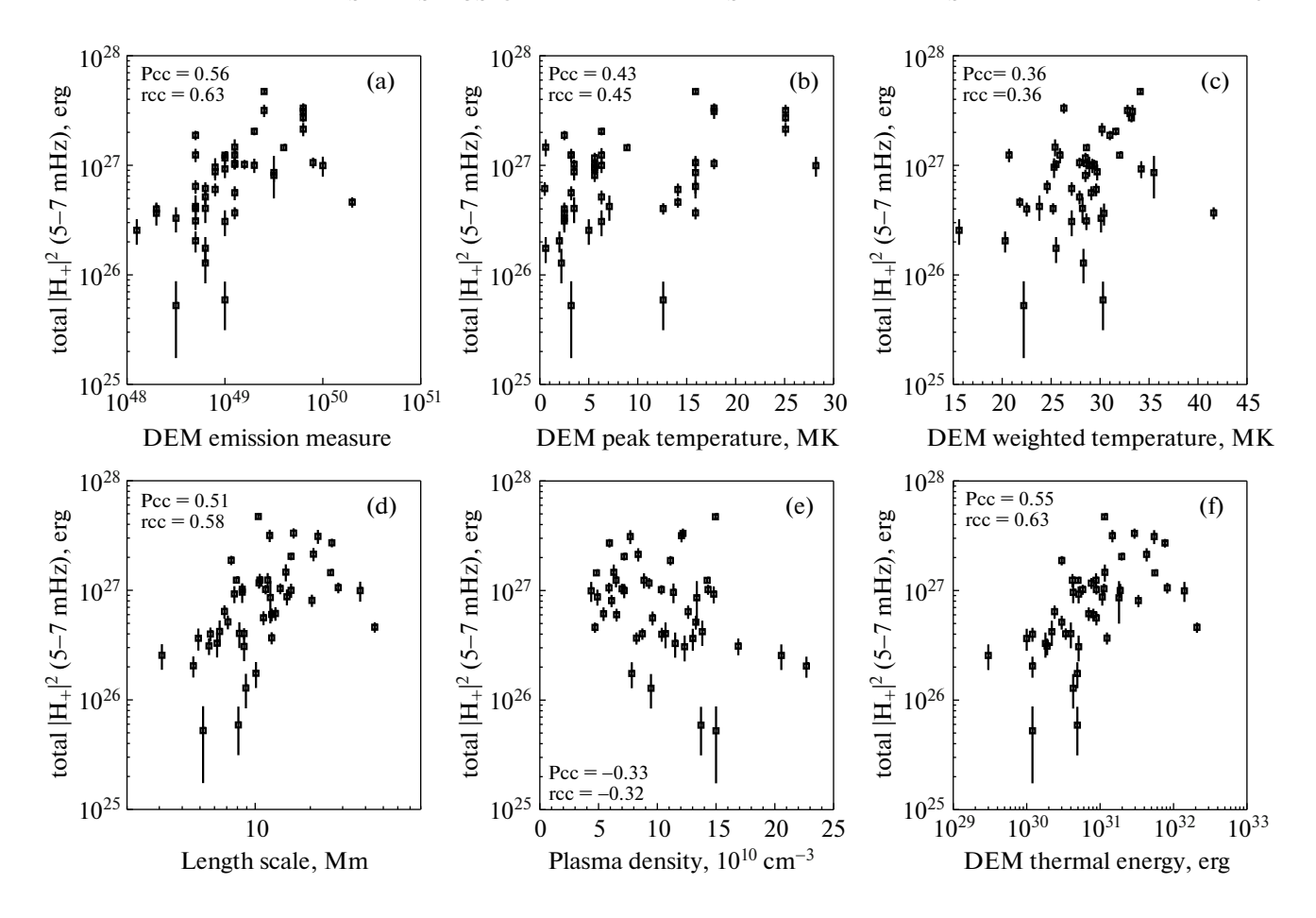


Fig. 7. Dependences of the total acoustic power of sunquakes for 22 flares in the frequency range 5–7 MHz on thermal plasma parameters (according to AIA data from GEII): (a) emission measure, (b) peak temperature according to DEM, (c) temperature obtained by averaging over DEM, (d) characteristic linear scale, (e) characteristic plasma concentration, (f) thermal energy. The Pearson correlation coefficient (Pcc) and rank correlation coefficient (rcc) values are indicated in the panels of the figure.

work of works [41, 42] showed the following main results:

- (1) the strongest correlation (according to Pearson 0.68) was obtained for the dependence of helioseismic energy on the total flux of non-thermal X-ray photons under the assumption of a fixed low-energy boundary of 20 keV;
- (2) an interesting result is the found correlation (0.58) of sunquake energy with plasma temperature according to RHESSI, with a weak correlation with the emission measure ($P_{cc} = 0.32$);
- (3) there is a clear dependence of the energy of sunquakes on the characteristic dimensions of the flare region. Thanks to this effect, we also observe a relationship ($P_{cc} = 0.56$) between helioseismic energy and the integral emission measure obtained from DEM analysis;
- (4) the DEM analysis did not allow us to find a good correlation between the energy of sunquakes and the plasma temperature ($P_{\rm cc} = 0.36$ and 0.43 for the temperatures $T_{\rm p}$ and $T_{\rm w}$), which contradicts the RHESSI data.

7. DISCUSSION OF THE RESULTS OBTAINED

Let us discuss the results obtained in relation to two important aspects: the physics of sunguakes and the methodology of statistical analysis. First of all, we note that from the point of view of statistical analysis, the potential of the SQ24 catalog is far from exhausted. When considering overlap with the GEII and GEVIII catalogs, we found, respectively, only 22 and 42 events before February 2014. When considering other flares after this date, we could expand the catalog for both DEM and X-ray analysis. However, RHESSI's germanium semiconductor detectors have undergone severe degradation since 2015. Therefore, very large and careful additional work is needed to interpret the X-ray spectrum of flares since 2015 (which was not done in the Global Energetics series). Note that for the purposes of the initial statistical analysis, we only need data without spatial resolution. In this regard, from our point of view, the next step would be to analyze the X-ray emission of a larger number of events using the KONUS instrument [46] on board the Wind spacecraft. This instrument is distinguished by the longest observation time compared to other X-ray spectrometers, the absence of eclipses and a relatively stable background. Analysis of expanded samples will make it possible to better compare flares with different degrees of photospheric activity and obtain refined correlations between the energy of sunquakes and the parameters of the X-ray non-thermal spectrum, which indirectly indicates accelerated electrons.

In this work, we used information on the characteristic linear dimensions of the flare region. Moreover, analysis of the distributions of characteristic lengths showed no differences between flares with sunguakes and flares without photospheric disturbances. However, we noticed that there is a correlation between the energy of sunquakes and the characteristic size of the flare region. In other words, we have shown that fast and pulsed flares with a helioseismic response [29] do not have the property of compact energy release regions from the point of view of the technique for estimating the characteristic sizes described in [42]. Nevertheless, the issue of the geometric structure of the flare region within the framework of studies of helioseismically active solar flares is not removed from the agenda and, moreover, is extremely important. In fact, this work only showed that in all flares the conditional number of magnetic loops (and their sizes) involved in the flare energy release is approximately the same. In this case, we do not consider the finer spatial structure of the flare region.

From the point of view of the hypothesis about the generation of helioseismic waves by accelerated electrons, one of the most important parameters is the area of their precipitation into the lower layers of the solar atmosphere. At different values of the area, the energy flux density of the precipitating accelerated electrons will also be different and, therefore, the photospheric response will be different. Based on the GEVIII catalog, we estimated the energy flux density of accelerated electrons and found a difference in the medians of the distributions (flares with solar quakes and flares without photospheric disturbances) by approximately five times (the same as in Fig. 4c). Also, the criteria used showed a significant difference in the distributions, despite the approximate estimate of the time of the pulse phase, the area of the flare region and the value of the low-energy boundary. Also, the estimate of the thermal plasma density depends on the refined geometric dimensions. Refinement of statistics in terms of geometric parameters in the future will significantly improve the understanding of helioseismically active solar flares. In addition, it is important to consider the multiplicity of compact areas of precipitation of accelerated particles, as well as the dynamics of the number and size of those areas into which accelerated electrons are injected (it is possible that successive injections can enhance the helioseismic wave).

One of the important results of the DEM analysis is the identity of samples of solar flares with sunquakes and without photospheric disturbances in terms of thermodynamic parameters. However, for the RHESSI data we found a difference in the medians of these distributions. Most likely, this is due to the construction of the DEM, which considers plasma in a very wide temperature range (from ~ 0.1 to ~ 20 MK). Note that, despite the high values of $T_{\rm w} = 6-40$ MK with a median of ~26 MK, exceeding the maximum temperature values according to RHESSI in the MK range $T_{\text{max}} = 0.5-25 \text{ MK}$ and a median of ~12 MK, the temperature data cannot be compared directly. The point is that T_{w} characterizes the DEM distribution as a whole, while the RHESSI temperature is determined from a single-temperature approximation of the X-ray spectrum at very short wavelengths with energies (about 5-20 keV) that are not actually accessible to AIA. AIA also has poor sensitivity to plasma radiation above 20 MK, while RHESSI reliably measures X-ray plasma radiation up to very high temperatures. It was shown in [47] that on average the ratio of flare plasma temperatures (for 149 M and X flares) according to RHESSI and AIA data is 1.9 \pm 0.1. We can say that in terms of diagnosing very hot plasma, we should trust the RHESSI data more. In connection with these considerations, it is tempting to consider the plasma, according to RHESSI X-ray measurements, to be more "directly" associated with the flare energy release region in which magnetic reconnection occurs. Whereas the plasma observed in the EUV range is determined to a greater extent by the effect of chromospheric evaporation and is therefore only indirectly related to the reconnection region in the corona. In other words, there is a large contribution to the total X-ray flux from hot plasma directly heated within (or in the vicinity of) the reconnecting current sheet (probable shock waves, turbulence, electric current dissipation, etc.). This issue should be studied in more detail in the future. Here, we only hypothesize why analyzes of AIA and RHESSI data may lead to different results.

We also note that as part of the analysis of thermal X-ray spectra using RHESSI data, it was found that the plasma density of flares with sunquakes is slightly higher (the medians differ by approximately three times) than for flares without photospheric disturbances, and there is also a correlation ($P_{cc} = 0.58$) between the energy of sunquakes and maximum plasma temperature. This may indirectly indicate that in helioseismically active solar flares there are more hot electrons in the tail of the Maxwellian distribution, which can be accelerated more efficiently. However, this statement is quite speculative, since the plasma density is determined in a specific way, and we do not know the details of the physics of acceleration. In the GEVIII catalog, the characteristic linear size is determined, as in GEII, based on the analysis of DEM maps (see above for more details). Generally speaking, considering the natural course of DEM, which is characterized by the fact that in the region of high temperatures (approximately more than 10 MK) there is less plasma, we can expect smaller volumes of plasma emitting X-ray bremsstrahlung. However, RHESSI does not provide images with a wide dynamic range and high (comparable to AIA) spatial resolution, and therefore we cannot estimate the real size of the hottest part of the flare region. Consequently, plasma density estimates from RHESSI are quite controversial. Because of this, we also did not present a graph of the correlation of helioseismic energy with plasma density according to RHESSI (however, the analysis showed that there is virtually no correlation). Thus, we again come to the importance of more accurately determining the geometric dimensions of flare regions, which is necessary for a better understanding of the characteristics of the energy release of helioseismically active flares.

Now let's move on to discussing the most important result of this article. Generally speaking, the statistical analysis performed indicates that the presence of increased fluxes of non-thermal X-ray radiation is a striking feature of helioseismically active solar flares. This indirectly indicates large fluxes of accelerated electrons compared to flares without a photospheric response. We also obtained a clear correlation (the best among other studied parameters) of helioseismic energy with X-ray fluxes. Based on these results, what prevents us from saying that the hypothesis of the generation of helioseismic disturbances by electrons falling into the lower layers of the solar atmosphere has been proven?

First, from a physics point of view, increased total (spatially integrated) fluxes of non-thermal X-ray radiation and, therefore, increased fluxes of accelerated electrons may be a secondary (accompanying) phenomenon in relation to some other more important parameter of flare energy release. Acceleration of charged particles most likely results from the exposure of electron populations to either large-scale or smallscale electric fields generated by magnetic reconnection and various instabilities of the reconnecting current sheet (in a wide variety of magnetic field geometries). Intense magnetic reconnection may be accompanied by other significant processes that may affect the lower layers of the solar atmosphere. For example, the eruptive process and magnetic field dynamics at the photosphere level may correlate with the rate of magnetic reconnection. The eruption itself may be the cause of magnetic reconnection during the pulse phase of a solar flare, stimulating rapid changes in the magnetic field in the lower layers of the solar atmosphere [48–50]. As a result of a magnetic field jump, a pulsed Lorentz force can arise, which is theoretically capable of generating photospheric disturbances (see Introduction). Also, in parallel with the acceleration of electrons, ions can be accelerated in the widest energy range. Moreover, ions may be a more preferable agent (due to their larger mass compared to electrons) for excitation of sunquakes [16]. Accordingly, increased fluxes of accelerated electrons may indirectly indicate in favor of accelerated ions, the very presence of which and their characteristics are extremely difficult to reliably establish from the available observational data. In future studies, the effect of accelerated MeV protons on the perturbation of the photosphere can be assessed by recording gamma radiation. However, there are no systematic observations of gamma-ray spectra yet, even in the "Sun as a star" observation mode.

Secondly, great uncertainty is introduced into the analysis by the transition from the description of fluxes of non-thermal X-ray radiation to fluxes of accelerated electrons and to an estimate of their total energy. We used the simplest "thick target" model [34]. However, in reality, the transport of accelerated particles can be much more complex, considering additional effects: capture in magnetic traps (for example, [51]), reverse electric current (for example, [51, 52]), small-scale turbulence (for example, [53]) and etc.

Also, the spectrum of X-ray radiation depends on the characteristics of the target: warm, thick, thin, partial ionization of the plasma, etc. It is almost impossible to take these effects into account within the framework of statistical analysis. Moreover, such a study is difficult to do even for individual solar flares. Additional distortions of the recorded hard X-ray radiation, complicating the interpretation of the spectrum, can be associated with the effect of Compton scattering (or albedo) from the photosphere (see, for example, [54]), which depends on the heliographic longitude and latitude of the flare.

A serious obstacle is the still insurmountable problem of uncertainty of the low-energy boundary above which the spectrum of accelerated electrons is integrated. Quite unexpectedly, we obtained a correlation ($P_{\rm cc}=0.51$) of non-thermal energy (within the "thick target" model) with the total energy of sunquakes, considering a very rough estimate of the low-energy boundary (we took the intersection of the thermal and non-thermal parts of the X-ray spectrum).

It is also worth noting that we have omitted in this section a discussion of the obvious importance of spatially resolved observations and the inclusion of other bands of the electromagnetic spectrum (particularly the microwave and gamma bands) in statistical analysis. There are so many problems here, that the description of which seems unnecessary and goes far beyond the scope of this article.

In conclusion, we would like to note that the obtained statistical results of the analysis of the characteristics of the energy release of helioseismically active solar flares are actually the first in the world. Conclusions drawn from the analysis of non-thermal

X-ray spectra so far provide only indirect evidence in favor of the hypothesis of the generation of sunquakes by accelerated electrons. Further extensive research is needed. We consider the results obtained in this article as a "seed" for our (and other authors') future statistical studies. First, it will be necessary to refine the results obtained for expanded samples of outbreaks. Secondly, improving methods in a number of areas (see discussion above) and connecting to statistical analysis of other parameters of solar flares (magnetic field, CME dynamics, etc.) will significantly improve the understanding of the conditions for the generation of sunquakes. Along with the analysis of observational data, it is necessary to develop modeling of sunquakes.

FUNDING

The presented work was supported by the Russian Science Foundation grant no. 23-72-30002.

CONFLICT OF INTEREST

The authors of the article declare that they have no conflicts of interest.

REFERENCES

- 1. C. L. Wolff, Astrophys. J. 176, 833 (1972).
- 2. A. G. Kosovichev and V. V. Zharkova, in *Helioseismology*, Ed. J. T. Hoeksema et al., ESA-SP **376**, 341 (1995).
- A. G. Kosovichev and V. V. Zharkova, Nature (London, U.K.) 393, 317 (1998).
- P. H. Scherrer, R. S. Bogart, R. I. Bush, et al., Solar Phys. 162, 129 (1995).
- V. Domingo, B. Fleck, and A. I. Poland, Solar Phys. 162, 1 (1995).
- C. Lindsey and D. C. Braun, Astrophys. J. 485, 895 (1997).
- A.-C. Donea, D. C. Braun, and C. Lindsey, Astrophys. J. Lett. 513, L143 (1999).
- 8. C. Lindsey and D. C. Braun, Solar Phys. **192**, 261 (2000).
- 9. J. C. Buitrago-Casas, J. C. Martínez Oliveros, C. Lindsey, et al., Solar Phys. **290**, 3151 (2015).
- 10. A. Donea, Space Sci. Rev. 158, 451 (2011).
- 11. A. G. Kosovichev, in *Extraterrestrial Seismology*, Ed. by V. Tong and R. García (Cambridge Univ. Press, Cambridge, 2015), p. 306.
- 12. A. G. Kosovichev, Solar Phys. **238**, 1 (2006).
- A. G. Kosovichev and T. Sekii, Astrophys. J. Lett. 670, L147 (2007).
- I. N. Sharykin, A. G. Kosovichev, V. M. Sadykov, I. V. Zimovets, and I. I. Myshyakov, Astrophys. J. 843, 67 (2017).
- 15. J. T. Stefan and A. G. Kosovichev, Astrophys. J. **895**, 65 (2020).
- V. M. Sadykov, J. T. Stefan, and A. G. Kosovichev, arXiv: 2306.13162 (2023).

- 17. S. Zharkov, L. M. Green, S. A. Matthews, and V. V. Zharkova, Astrophys. J. Lett. **741**, L35 (2011).
- S. Zharkov, L. M. Green, S. A. Matthews, and V. V. Zharkova, Solar Phys. 284, 315 (2013).
- 19. H. S. Hudson, G. H. Fisher, and B. T. Welsch, *Subsurface and Atmospheric Influences on Solar Activity*, Ed. by R. Howe, ASP Conf. Ser. **383**, 221 (2008).
- 20. G. H. Fisher, D. J. Bercik, B. T. Welsch, and H. S. Hudson, Solar Phys. **277**, 59 (2012).
- 21. J. D. Alvarado-Gómez, J. C. Buitrago-Casas, J. C. Martínez-Oliveros, et al., Solar Phys. **280**, 335 (2012).
- 22. O. Burtseva, J. C. Martínez-Oliveros, G. J. D. Petrie, and A. A. Pevtsov, Astrophys. J. **806**, 173 (2015).
- A. J. B. Russell, M. K. Mooney, J. E. Leake, and H. S. Hudson, Astrophys. J. 831, 42 (2016).
- I. N. Sharykin, A. G. Kosovichev, and I. V. Zimovets, Astrophys. J. **807**, 102 (2015).
- 25. I. N. Sharykin and A. G. Kosovichev, Astrophys. J. **808**, 72 (2015).
- 26. D. Besliu-Ionescu, A. Donea, and P. Cally, Sun Geosphere 12, 59 (2017).
- R. P. Lin, B. R. Dennis, G. J. Hurford, et al., Solar Phys. 210, 3 (2002).
- 28. R. Chen and J. Zhao, Astrophys. J. 908, 182 (2021).
- I. N. Sharykin and A. G. Kosovichev, Atrophys. J. 895, 76 (2020).
- 30. P. H. Scherrer, J. Schou, and R. I. Bush. Solar Phys. **275**, 207 (2012).
- 31. W. D. Pesnell, B. J. Thompson, and P. C. Chamberlin, Solar Phys. **275**, 3 (2012).
- 32. W. M. Neupert, Astrophys. J. Lett. 153, L59 (1968).
- 33. B. R. Dennis and D. M. Zarro, Solar Phys. **146**, 177 (1993).
- 34. J. C. Brown, Solar Phys. 18, 489 (1971).
- 35. M. A. Livshits, O. G. Badalian, A. G. Kosovichev, and M. M. Katsova, Solar Phys. 73, 269 (1981).
- G. H. Fisher, R. C. Canfield, and A. N. McClymont, Astrophys. J. 289, 414 (1985).
- 37. A. G. Kosovichev, Bull. Crimean Astrophys. Observ. **75**, 6 (1986).
- 38. J. C. Allred, A. F. Kowalski, and M. Carlsson, Astrophys. J. **809**, 104 (2015).
- 39. H. Wu, Y. Dai, and M. D. Ding, Astrophys. J. Lett. **943**, L6 (2023).
- 40. J. R. Lemen, A. M. Title, D. J. Akin, et al., Solar Phys. **275**, 17 (2012).
- 41. M. J. Aschwanden, E. P. Kontar, and N. L. S. Jeffrey, Astrophys. J. **881**, 22 (2019).
- 42. M. J. Aschwanden, P. Boerner, D. Ryan, et al., Astrophys. J. **802**, 53 (2015).
- 43. M. J. Aschwanden, G. Holman, A. O'Flannagain, et al., Astrophys. J. 832, 27 (2016).
- 44. E. P. Kontar, N. L. S. Jeffrey, A. G. Emslie, and N. H. Bian, Astrophys. J. **809**, 35 (2015).

- 45. M. J. Aschwanden, P. Boerner, A. Caspi, et al., Solar Phys. **290**, 2733 (2015).
- R. L. Aptekar, D. D. Frederics, and S. V. Golenetskii, Space Sci. Rev. 71, 265 (1995).
- 47. D. F. Ryan, A. M. O'Flannagain, M. J. Aschwanden, and P. T. Gallagher, Solar Phys. **289**, 2547 (2014).
- 48. G. J. D. Petrie, Astrophys. J. 759, 50 (2012).
- 49. S. Wang, C. Liu, R. Liu, N. Deng, Y. Liu, and H. Wang, Astrophys. J. Lett. **745**, L17 (2012).
- I. N. Sharykin, I. V. Zimovets, and A. V. Radivon, Cosmic Res. 61, 265 (2023).

- A. N. Shabalin, Yu. E. Charikov, and I. N. Sharykin, Astrophys. J. 931, 27 (2022).
- 52. V. V. Zharkova and M. Gordovskyy, Astrophys. J. **651**, 553 (2006).
- Yu. E. Charikov and A. N. Shabalin, Tech. Phys. 66, 1092 (2021).
- 54. E. P. Ovchinnikova, Yu. E. Charikov, A. N. Shabalin, and G. I. Vasil'ev, Geomagn. Aeron. 58, 1008 (2018).

Publisher's Note. Pleiades Publishing remains neutral with regard to jurisdictional claims in published maps and institutional affiliations.